JOURNAL OF MATERIALS SCIENCE **33** (1998) 4937 – 4942

Hollow alumina microspheres from boehmite sols

M. CHATTERJEE, D. ENKHTUVSHIN*, B. SILADITYA, D. GANGULI
Sol–Gel Division, Central Glass & Ceramic Research Institute, Calcutta 700 032, India
E-mail: dganguli@cscgeri.ren.nic.in

Hollow alumina microspheres were obtained from emulsified boehmite sols by an ion extraction method. The viscosity and the equivalent alumina content of the sols were found to affect the characteristics of the derived microspheres. High-viscosity sols produced broken microspheres. A temperature of about 400–500 °C for boehmite to γ-Al_2O_3 transformation in the gel microspheres was observed by differential thermal analysis and X-ray diffraction. Complete crystallization of the gel microspheres to α-Al_2O_3 occurred at 1200 °C. A tentative mechanism for the formation of the hollow microspheres is presented.

1. Introduction

Hollow microspheres of ceramic and glass compositions find a large number of applications varying from conventional uses like thermal insulation to special ones like inertial confinement fusion of nuclear materials [1, 2]. Various methods of producing such microshells have been discussed by Wilcox and Berg [3]. Of these, the emulsion–water extraction method starting from colloidal sols has been studied recently in detail [1].

In the present work, an ion extraction technique has been employed (instead of water extraction) for obtaining hollow microspheres of alumina from emulsified colloidal alumina sols. The main advantages of the process are the relatively high yield and small reaction time. In the following, the conditions of hollow sphere formation and the geometrical characteristics of the products as a function of experimental parameters are described.

2. Experimental procedure

2.1. Preparation of an alumina sol

For the preparation of a parent aqueous alumina sol, $Al(NO_3)_3.9H_2O$ was used as the starting material. Boehmite particles were precipitated from the aluminium nitrate solution at 80–90 °C with an ammonia solution. The washed precipitate was peptized with glacial acetic acid at 80–90 °C to obtain a colloidal sol. The pH, viscosity and Al_2O_3-content of the parent sol were 4.91, 3.7–3.9 mPa.s and 1.00 M respectively. From this parent sol, several sols of different viscosities were prepared by evaporation (Table I).

2.2. Preparation of emulsions

Water-in-oil (W/O) type emulsions were used in the present investigation. The sols prepared as in Section 2.1 above were used as the aqueous phase. An organic liquid, 1,1,1trichloroethane (TCE) or *n*-heptane containing 2–2.5 vol % (with respect to the organic liquid) of a surfactant, e.g. Span 80 (Fluka) with HLB (hydrophilic/lipophilic balance) value of 4.3 acted as the support solvent, i.e. the oil phase. The emulsions were prepared by dispersing the colloidal sol as droplets in the support solvent under constant agitation. The volume ratio of the sol : support solvent was kept constant at 1 : 4 in all experiments.

2.3. Preparation of gel and oxide microspheres

The emulsified sol droplets were converted to gel spheres by the addition of an organic amine (extractant or gelling agent), e.g. triethylamine [4, 5] under agitation until a pH of 8–9 was reached. The volume ratio of the sol to gelling agent was about 1 : 0.4. The gel microspheres were separated by filtration, washed with acetone and methanol and finally dried at 110 °C. The characteristics of the sols and the gel microspheres have been presented in Table I.

The gel microspheres corresponding to Run no. 4 of Table I were calcined at specific temperatures in the range 100–1200 °C under static condition, each with 1 h soak, while those of Run nos. 3 and 6 were calcined only at 1200 °C with 1 h soak for examining the effect of viscosity of the sols on the powder characteristics.

2.4. Characterization of the products

The boehmite precipitate, dried at 100 °C (precursor material), was characterized by differential thermal analysis (DTA; 404 Netzsch), Fourier transform infrared (FTIR) study (Nicolet 5 pc), X-ray diffraction (XRD; Philips PW-1730 X-ray unit) with Ni-filtered CuK_α radiation and transmission electron microscopy (TEM; Jeol, JEM–200 X). A small portion of the peptized sol was evaporated to dryness at 100 °C and the peptized material was characterized by XRD and TEM.

---

*Trainee from New Material and Chemical Technology Centre of Mongolian National University, Mongolia during the period October 1994 to August 1995.

TABLE I Characteristics of the sols and the oxide particles at 1200 °C/1 h

Run no.	Span 80 (vol %)	Viscosity mPa.s	Optical microscopic results
1.	2.0	14–15	Mostly large broken spheroids
2.	2.0	21–22	Mostly broken spheres + irregular shaped materials
3.	2.5	10–12	Almost all spheres
4.	2.5	15–16	Almost all spheres
5.	2.5	20–21	Mostly spheres + very little broken spheres
6.	2.5	25–26	Spheres + broken spheres
7.	2.5	28–30	Mostly large broken spheres

The gel and calcined microspheres were characterized by DTA and thermogravimetry, TG (TA 501), FTIR study, XRD, optical microscopy (Leitz, Ortholux, II POL-BK), scanning electron microscopy (SEM; S 250 and S 430) and particle size analysis (Sedigraph MM5100, Micromeritics). Powder density of the oxide microspheres (obtained at 1300 °C/1h) of Run 4 of Table I was determined using Archimedes' principle.

3. Results and discussion

3.1. Formation of the spherical particles

Under the present conditions of precipitation, poorly crystalline boehmite was identified by XRD in the precursor material. Fig. 1 shows the transmission electron micrograph (TEM) of the as-precipitated, dried (at 100 °C) boehmite particles. The particles were found to be highly agglomerated. Peptization of the particles with acetic acid produced a semitransparent sol. Fig. 2 presents a TEM of the powder obtained after drying a small portion of the peptized sol at 100 °C. The figure clearly indicates that the particle size of the precipitated boehmite was considerably reduced after peptization. XRD also shows the retainment of the poorly crystalline boehmite particles in the peptized powder.

Table I presents the nature of the oxide particles obtained from sols of different viscosities. Addition of 2.5 vol % of Span 80 was found to be sufficient for obtaining good microspheres. A surfactant concentration of less than 2.5 vol % was not effective for sphere formation. The formation of gel microspheres may be explained to be caused by the adsorption of the surfactant molecules at the interface of the sol droplets and the support solvent, causing a decrease in the interfacial tension, increasing the stability of the droplets by steric hindrance and thereby preventing their coalescence [6]. A volume ratio of the sol to the gelling agent (extractant) of about 1 : 0.4 in the present method (in contrast to the water extraction technique [1] where the above ratio was 1 : 15) helped to increase the yield of the product in a fixed volume.

TABLE II DTA results of the precursor material and gel microspheres

Sample no.	Peak temperature (°C) Endothermic	Exothermic
B1	150 270 310	490
B2	190 300	410 520

3.2. Thermal analysis

DTA results of the precursor material (Sample no. B1) and those of gel spheres (sample no. B2) derived from the sol (dried at 100 °C) from ambient temperature to 1000 °C, have been presented in Table II. The appearance of several endothermic peaks in the temperature range of 150 to 310 °C for both the samples can be assigned to the expulsion of loosely bound water molecules associated with the materials and some decomposition products, e.g. residual nitrates (for sample no. B1), acetates and other organics (for sample no. B2) [7, 8]. The broad and small exothermic peaks at 490 °C and 410 °C for B1 and B2, respectively, indicate the crystallization of γ-Al_2O_3 [7, 9]. The relatively low crystallization temperature of γ-Al_2O_3 for B2 may be attributed to its smaller particle size [10, 11] (prepared from peptized sol) than that of B1.

Formation of δ-Al_2O_3 in sample no. B2 is considered to be the reason of appearance of the second broad and

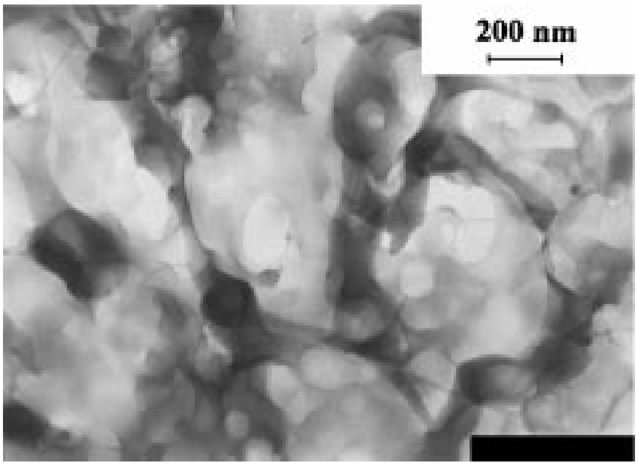

Figure 1 Transmission electron micrograph of the boehmite precursor dried at 100 °C.

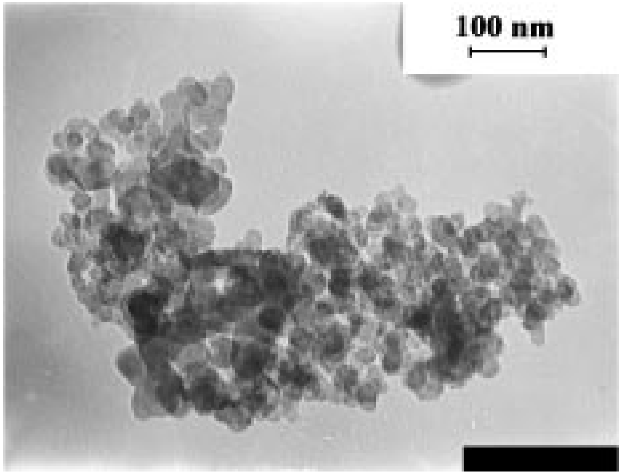

Figure 2 Transmission electron micrograph of the peptized particles obtained after drying (at 100 °C) the parent boehmite sol.

TABLE III Absorption bands in the FTIR spectra of the precursor material and gel microspheres at different temperatures

Sample no.	Absorption bands (cm^{-1})								
B1	3490	2395	1763	1636		1385	963		592
B2	3472	2380		1633	1420				563
B3	3472	2380		1584	1424			609	
B4	3449	2363		1630					592

weak exotherm at 520 °C. This can be supported from the XRD results, as discussed in Section 3.4. No other peaks were observed during heating up to 1000 °C. A similar thermal behaviour of the precursor material and the gel microspheres derived from the peptized product is obvious from the above results.

During heat-treatment from ambient temperature to 1300 °C, TG of sample no. B2 showed a total weight loss of about 44% of which a sharp decrease in weight (28%) was noted up to 297 °C. Removal of loosely bound water molecules and most of the volatiles occurred around this temperature. The result is comparable with that obtained from DTA. A further weight loss of 14.5% was noted up to 573 °C; this occurred by the expulsion of residual acetate and water molecules formed by the dehydroxylation of the material [9]. An insignificant weight loss of 1.5% from 573 to 1300 °C was caused by the removal of the last traces of water molecules generated by dehydroxylation and residual carbon via oxidation.

3.3. FTIR spectroscopic study

To examine the characteristics of the products calcined at different temperatures, FTIR spectra of the four samples B1 (precursor material), B2, B3 and B4 (gel microspheres heat-treated at 100, 400 and 1200 °C, respectively) were recorded in the wave number range 400–4000 cm^{-1}. The major absorption bands identified are summarized in Table III.

The bands at around 3449–3490 cm^{-1} and 1584–1636 cm^{-1} appeared in all the samples; these are considered to be due to the stretching vibrations of H-bonded hydroxyls and molecular water respectively [7, 12]. The intensities of these bands went on decreasing with increase in the calcination temperature, obviously caused by the gradual removal of water molecules. Absorbed CO_2 produced a band at around 2363–2395 cm^{-1} [12]. Absorption bands centred at 1763 cm^{-1} and 1385 cm^{-1} are assigned to the presence of residual nitrate groups [13, 14] in the precursor material (sample no. B1). The absence of these bands in the gel microspheres (sample no. B2) indicates the removal of the last traces of nitrate groups after repeated washing with acetone and methanol (Section 2.3). Again, acetate groups in sample nos. B2 and B3 generated very small absorption bands at 1420 cm^{-1} and 1424 cm^{-1} [14]. The absence of the acetate groups was confirmed in sample no. B4, calcined at 1200 °C. Different types of vibrations for the Al–O and Al–OH bands were observed in the samples at around 963, 609, 592 and 563 cm^{-1} [7, 15].

TABLE IV Crystal phases in the oxide microspheres at different temperatures

Run no.	Calcination temperature (°C)	Crystal phases by XRD
1.	100	Boehmite
2.	200	Boehmite
3.	400	Boehmite + γ-Al_2O_3 (minor)
4.	600	γ-Al_2O_3 + δ-Al_2O_3 (minor)
5.	800	δ-Al_2O_3 + γ-Al_2O_3
6.	1000	δ-Al_2O_3 + γ-Al_2O_3 + θ-Al_2O_3 (little)
7.	1100	θ-Al_2O_3 + δ-Al_2O_3 (little)
8.	1200	α-Al_2O_3

3.4. Crystallization behaviour of the microspheres

Crystalline phases identified by XRD in microspheres calcined at different temperatures have been presented in Table IV. XRD of the gel spheres, dried at 100 °C, showed the expected presence of boehmite. Because of the poorly crystalline nature of the sample, the XRD peaks were broad and small. This indicates the identical nature of the precursor material and gel microspheres derived from it. The phase pure boehmite was found to persist when the gel microspheres were heat-treated at 200 °C.

At 400 °C, γ-Al_2O_3 appeared in minor quantity. The formation of γ-Al_2O_3 was also indicated in the DTA curve at 410 °C (exothermic peak) for the same sample. δ-Al_2O_3 appeared when the calcination temperature was between 400 and 600 °C. This supports the appearance of the second exothermic peak at 520 °C in the DTA curve. θ-Al_2O_3 appeared at 1000 °C and persisted as the major phase at 1100 °C. α-Al_2O_3 was identified as the single phase at 1200 °C. So, the pathway of crystallization of the precursor boehmite gel microspheres may be indicated as follows

$$\text{Boehmite} \rightarrow \gamma\text{-}Al_2O_3 \rightarrow \delta\text{-}Al_2O_3 \rightarrow \theta\text{-}Al_2O_3 \rightarrow \alpha\text{-}Al_2O_3$$

Similar transformation behaviour was observed by previous workers during crystallization of aluminium hydrous oxides [9, 16, 17].

3.5. Optical and scanning electron microscopy (SEM)

The morphology of the products obtained under different conditions (Table I) was checked with an optical microscope. Such investigations revealed that the powders

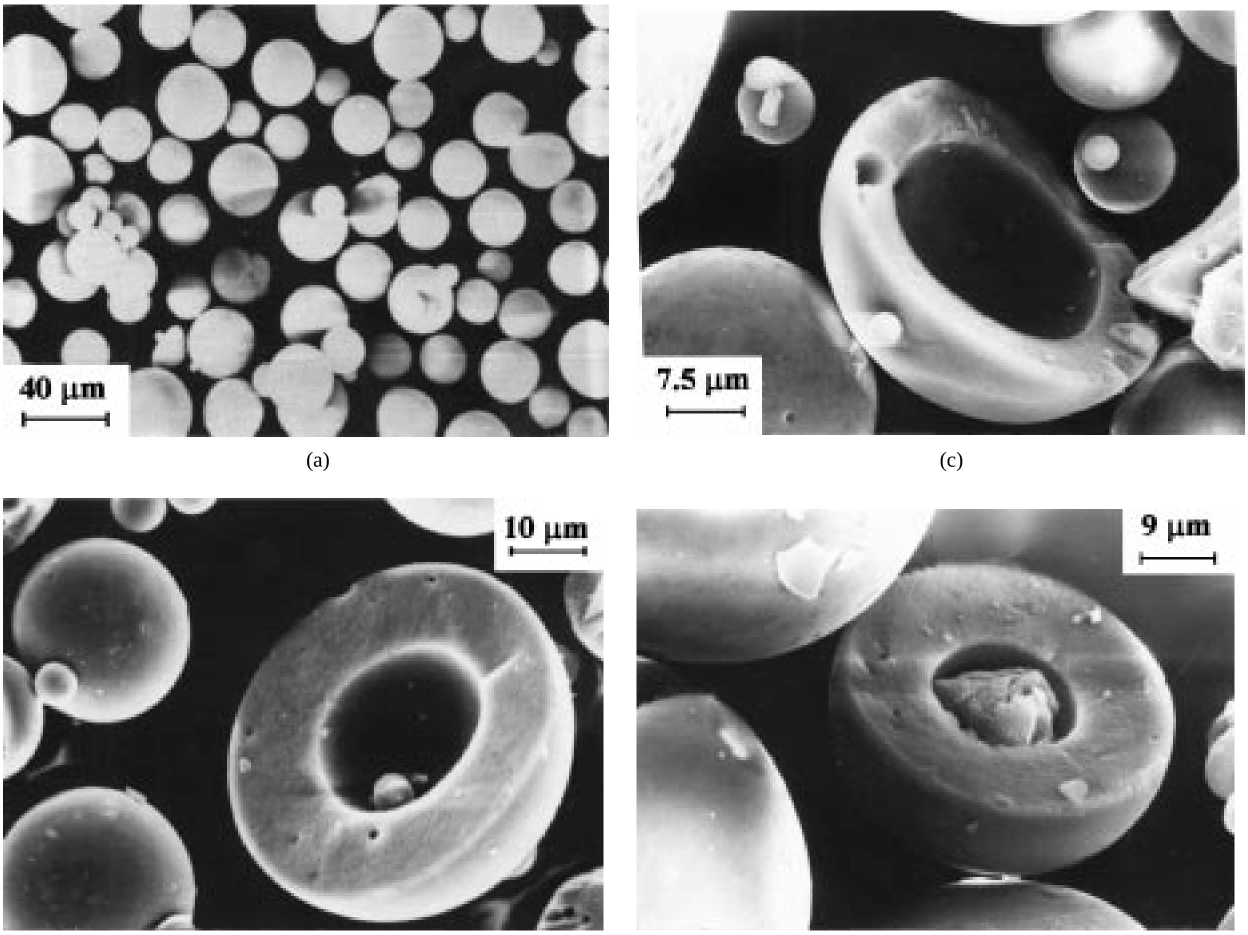

(a) (c)

(b) (d)

Figure 3 (a) Scanning electron micrograph showing the morphology of crystallized (α-Al_2O_3) microspheres calcined at 1200 °C/1 h (Product of Run no. 4 of Table I). (b) Scanning electron micrograph of a fractured hollow microsphere of α-Al_2O_3 with a single pore obtained at 1200 °C/1 h (Product of Run no. 4 of Table I). (c) Scanning electron micrograph of α-Al_2O_3 (calcined at 1200 °C/1 h) showing small unbroken microspheres along with a large broken hollow microsphere with a single spherical cavity (Product of Run no. 6 of Table I). (d) Scanning electron micrograph showing the presence of a highly agglomerated, irregular shaped residual material trapped within the spherical cavity of a fractured α-Al_2O_3 microsphere (Product of Run no. 6 of Table I).

generated by the sol-gel route were spherical in shape and the sphericity was retained even after calcination at 1200 °C/1 h (for Run nos. 3 and 4).

The oxide microspheres of Run nos. 4 and 6, both calcined at 1200 °C, of Table I were examined under SEM. The following observations are made.

1. The oxide microspheres of Run no. 4, derived from a sol of low viscosity, i.e. 15–16 mPa.s, were mostly spherical in morphology (Fig. 3a) and contained very few hollow broken particles (Fig. 3b). The particles contained a single spherical pore. The fractured microspheres did not contain any remnant particle in the internal hollow part.
2. The oxide microspheres of Run no. 6. derived from a sol of high viscosity, i.e. 25–26 mPa.s showed the following features.
   - (i) Microspheres of size up to about 20 μm did not break, but those larger than 20 μm were found to be mostly broken (Fig. 3c).
   - (ii) The fractured microspheres were observed to be hollow with a single spherical cavity (Fig. 3c).
   - (iii) In some cases, the fractured microsphere contained a highly agglomerated, irregular-shaped residual material trapped within the spherical cavity of the particle (Fig. 3d).

3.6. Particle size distribution

Oxide microspheres obtained from Run nos. 3, 4, and 6 of Table I, all calcined at 1200 °C/1 h, were studied for their size distribution as a function of the viscosity of the starting sol. The average particle size (d_{50}) of the product of Run no. 3 was 19 μm, while those of Run nos. 4 and 6 gave about the same value, i.e. 22 μm (Fig. 4). Spheres obtained from the sols of the lower viscosity and the lowest equivalent Al_2O_3 concentration were the smallest in size. Thus, under a given speed of agitation, sols of lower equivalent oxide concentration and lower viscosity, i.e. low degree of polymerization, can be effectively broken into smaller droplets which after gelation and subsequent calcination ultimately produced smaller microspheres [1].

Although the d_{50} values of Run nos 4 and 6 are the same, the particle size distribution of the product of Run no. 6 was to an extent wider, particularly in the lower range (below 20%) than that of the powder of

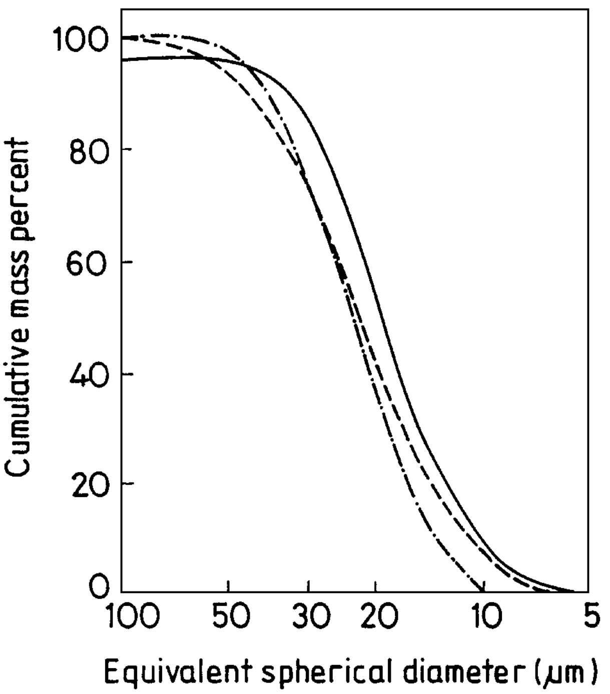

Figure 4 Particle size distribution of the oxide microspheres calcined at 1200 °C/1 h.(——) Product of Run no. 3 of Table I; (–·–) Product of Run no. 4 of Table I; (– –) Product of Run no. 6 of Table I.

Run no. 4. This difference may be a result of the high value of the viscosity of the sol causing breakdown of some of the gel microspheres into smaller particles. Observation under SEM supports this fact (Fig. 3c and d). The cause of breakdown of the microspheres has been explained in Section 4.

4. Tentative mechanism for the formation of hollow microspheres

In order to establish a mechanism of the formation of hollow microspheres in the present study, gel formation occurring in a single sol droplet is considered below. Ion exchange starts as soon as the base, i.e. triethylamine (TEA) is added. The extraction can be taken as complete when, on addition of TEA, the pH rises to 8–9. The ion extraction may be assumed to take place in three different steps (18):

1. Dissolution of TEA in organic phase, i.e. 1,1,1-trichloroethane (TCE);
2. Diffusion of TEA to the organic/aqueous interface; and
3. Formation of triethylamine acetate, $(C_2H_5)_3N.HOAc$, at the interface according to the reaction [19, 20]

$$(C_2H_5)_3N_{(org)} + H^+_{(aq)} \rightleftharpoons (C_2H_5)_3N^+H_{(interface)}$$

$$(C_2H_5)_3N^+H_{(interface)} + OAc^-_{(aq)}$$
$$\rightleftharpoons (C_2H_5)_3N^+H\,OAc^-_{(org)}$$

As soon as the sol droplets come in contact with TEA, rapid removal of both H^+ and OAc^- takes place from the outer surface of the droplet. This ion extraction is also believed to occur by the removal of water molecules close to the droplet surface [20]. At this stage, (i) depletion of water from the surface region of the sol droplets, and (ii) shrinkage of the sol droplets may be expected, resulting in the development of a concentration gradient of the colloid particles, being greater at the droplet surface than in the central region [1]. When the surface concentration of the colloid reaches a critical value, the formation of a gel network or "shell" on the outermost surface of the sol droplets occurs.

During the course of the reaction, as the water of the enclosed sol droplets diffuses through the porous shell towards the outer organic phase where TEA is continuously added, deposition of the colloidal particles takes place on the inner surface of the shell, causing its growth. As water comes out, the organic phase, i.e. TCE with a linear structure is expected to counterdiffuse rather easily through the shell, forming an aquo-organic liquid-filled gel microcapsule. On the other hand, diffusion of the bulky TEA molecules [19] through the shell becomes slow, so that growth of the shell is stopped after a certain stage in some droplets (Fig. 3d). This depends on the readily built up shell thickness, viscosity of the sol, the colloid concentration and concentration gradient as a function of time in the sol droplet etc. When the droplet size is small, the shell formation can continue up to the centre, so as to give a non-hollow gel sphere.

In case of the microspheres obtained from the low viscosity and low equivalent Al_2O_3 sol, the shell formation with less dense network and high permeability to both TEA and TCE is believed to occur towards the interior part of the droplet, making the shell formation process complete. During repeated washing of these microcapsules through a Buchner system under vacuum with methanol and acetone (Section 2.3), the trapped liquid is expected to come out gradually with the washing solvent through the highly permeable shell. Final removal of the washing solvent under vacuum forms gel microspheres with the internal cavity devoid of any trapped liquid, or containing negligible amount of liquid.

During calcination of the washed gel microspheres, the trapped liquid, if any, vaporizes and the vapours may be expected to get a passage for their removal through the permeable shell. Under such conditions, formation of unbroken and hollow oxide microspheres takes place [21, 22] (Fig. 1). Powder density of this batch (calcined at 1300 °C/1 h) containing essentially α-Al_2O_3, measured according to Archimedes' principle, was 3.42 g cm^{-3}, i.e. 86% of the theoretical density. This was much lower than that (98% of theoretical) recorded for α-Al_2O_3 microspheres prepared by the polymerization of a $Al(NO_3)_3$ solution at 80–90 °C with an ammonia solution and calcined at the same temperature [5]. It is thus an indication that these unbroken particles were also hollow [21].

In case of microspheres obtained from a sol of high viscosity and high equivalent Al_2O_3 concentration, formation of a dense and low permeable shell is believed to occur after complete shell formation. In some cases, such dense shell may prevent the diffusion of bulky TEA through it after a certain course of the reaction. This can give rise to a microcapsule with a part of the entrapped sol (Fig. 3d). Gel microcapsules, prepared from such sols, during washing as described earlier, failed to remove most of the trapped liquid or the entrapped sol through the low permeable dense shell. During calcination of these microcapsules, the escape of the volatiles formed from the entrapped liquid is expected to be hindered, thus giving rise to a build-up of internal pressure causing fracture of the microspheres [21–23] (Fig. 3c). In case of the gel microspheres with the entrapped sol, calcination not only leads to the breakdown of the microspheres, but the formation of highly agglomerated irregular shaped particles enclosed in the spherical cavity (Fig. 3d). Microspheres of size less than 20 μm did not break. The particles may be either solid or may contain little porosity [21, 23].

5. Conclusions

1. A boehmite sol was obtained by peptization of the precursor boehmite precipitate with glacial acetic acid at 80–90 °C. The retainment of crystallinity of the boehmite precipitate after peptization was confirmed by XRD. The gel microspheres were obtained from emulsified boehmite sols by an ion extraction method. Calcination of the gel microspheres at 1200 °C produced hollow α-Al_2O_3 microspheres.

2. The boehmite precursor, gel and the calcined microspheres were characterized by DTA, TG, FTIR, optical microscopy, TEM and SEM. Crystallization of γ-Al_2O_3 at about 400 °C in the gel microspheres was confirmed by DTA and XRD. Formation of α-Al_2O_3 took place through the formation of several transient phases of alumina.

3. The spherical morphology of the gel and the calcined particles was confirmed by optical and scanning electron microscopy. Formation of hollow microspheres was identified by SEM. A tentative mechanism of formation of the hollow microspheres has been described, which explains the microscopic observations.

Acknowledgements

The authors thank members of the Technical Ceramics, Electroceramics, Refractories, SEM and ESCA and finally X-ray Division for characterization of the powders.

References

1. J. G. LIU and D. L. WILCOX, SR., *J. Mater. Res.* **10** (1995) 84.
2. R. L. DOWNS, M. A. EBNER and W. J. MILLER, in "Sol-gel technology for thin films, fibres, preforms, electronics and specialty shapes," edited by L. C. Klein (Noyes Publications, Park Ridge, USA, 1988) p. 330.
3. D. L. WILCOX SR. and M. BERG, in "Hollow and solid spheres and microspheres: science and technology associated with their fabrication and application," edited by D. L. Wilcox Sr., M. Berg, T. Bernat, D. Kellerman and J. K. Cochran, Jr.; Mater. Res. Soc. Symp. Proc., Vol. 372 (Materials Research Society, Pittsburgh, Pennsylvania, 1995) p. 3.
4. M. CHATTERJEE, J. RAY, A. CHATTERJEE, D. GANGULI, S. V. JOSHI and M. P. SRIVASTAVA, *J. Mater. Sci.* **28** (1993) 2803.
5. J. RAY, M. CHATTERJEE and D. GANGULI, *J. Mater. Sci. Lett.* **12** (1993) 1755.
6. D. GANGULI and M. CHATTERJEE, "Ceramic powder preparation: a handbook" (Kluwer Academic Publishers, Boston, USA, 1997) p. 57.
7. T. SATO, S. IKOMA and F. OZAWA, in Proceedings of the Seventh International Conference on Thermal Analysis, Vol. I, edited by B. Miller (John Wiley & Sons, Chichester, New York, 1982) p. 450, 578.
8. F. W. DYNYS and J. W. HALLORAN, *J. Amer. Ceram. Soc.* **65** (1982) 442.
9. T. V. MANI, P. K. PILLAI, A. D. DAMODARAN and K. G. K. WARRIER, *Mater. Lett.* **19** (1994) 237.
10. K. N. P. KUMAR, K. KEIZER, A. J. BURGGRAAF, T. OKUBO, H. NAGAMOTO and S. MOROOKA, *Nature* **358** (1992) 48.
11. Y. S. BYOUN, C. S. OH and S. C. CHOI, in "Ceramic transactions," Vol. 51, Ceramic Processing Science and Technology, edited by H. Hausner, G. L. Messing and S. Hirano (The American Ceramic Society, Westerville, Ohio, 1995) p. 21.
12. C. MORTERRA, C. EMANUEL, G. CERRATO and G. MAGNACCA, *J. Chem. Soc. Faraday Trans.* **88** (1992) 339.
13. K. NAKAMOTO, "Infrared and Raman spectra of inorganic and co-ordination compounds" (Wiley, New York, 1978).
14. K. KAMIYA, K. TAKAHASHI, T. MAEDA, H. NASU and T. YOKO, *J. Eur. Ceram. Soc.* **7** (1991) 295.
15. MALGORZATA SOPICKA-LIZER, in "Euro-ceramics," Vol 1, edited by G. de With, R. A. Terpstra and R. Metselaar (Elsevier Applied Science, London, 1989) p. 1609.
16. W. H. GITZEN (Ed.), "Alumina as a ceramic material" (The American Ceramic Society, Columbus, Ohio, 1970), p. 17.
17. H. P. ROOKSBY, in "The X-ray identification and crystal structures of clay minerals," edited by G. Brown (Mineralogical Society, Clay Minerals Group, London, 1961) p. 354.
18. M. AKINC and A. CELIKKAYA, in "Advances in ceramics," Vol. 21, Ceramic Powder Science, edited by G. L. Messing, K. S. Mazdiyasni, J. W. McCauley and R. A. Haber (The American Ceramic Society, Westerville, Ohio, 1987) p. 57.
19. I. L. FINAR, "Organic chemistry" Vol. 1 (The English Language Book Society and Longman Group Limited, London, 1973) p. 373.
20. J. L. WOODHEAD, *J. Mater. Educ.* **6** (1984) 887.
21. G. PRAVDIC and M. S. J. GANI, *J. Mater. Sci.* **31** (1996) 3487.
22. G. L. MESSING, S.-C. ZHANG and G. V. JAYANTHI, *J. Amer. Ceram. Soc.* **76** (1993) 2707.
23. S.-C. ZHANG, G. L. MESSING and M. BORDEN, *ibid.* **73** (1990) 61.

Received 5 January
and accepted 14 July 1998